SpikeShip: A method for fast, unsupervised discovery of high-dimensional neural spiking patterns

Boris Sotomayor-Gómez[1,2], Francesco P. Battaglia[3], Martin Vinck[1,2,*]

1 Ernst Strüngmann Institute (ESI) for Neuroscience in Cooperation with Max Planck Society, Frankfurt, Germany
2 Donders Centre for Neuroscience, Department of Neuroinformatics, Radboud University Nijmegen, Nijmegen, Netherlands
3 Donders Institute for Brain, Cognition and Behaviour, Radboud University Nijmegen, Nijmegen, Netherlands

* martin.vinck@esi-frankfurt.de

Abstract

Neural coding and memory formation depend on temporal spiking sequences that span high-dimensional neural ensembles. The unsupervised discovery and characterization of these spiking sequences requires a suitable dissimilarity measure to compare any two spiking patterns. Here, we present a new measure of dissimilarity between multi-neuron spike sequences based on optimal transport theory, called *SpikeShip*. SpikeShip compares any two spiking patterns based on all the relative spike-timing relationships among neurons. Specifically, SpikeShip computes the optimal transport cost, i.e. the Earth Mover's Distance, to make all the relative spike-timing relationships (across neurons) identical between two spiking patterns. It achieves this by computing the optimal transport of spikes across time, per neuron separately, and then decomposing this transport cost in a temporal rigid translation term and a vector of neuron-specific transport flows. We show that SpikeShip can be effectively computed for high-dimensional neuronal ensembles, has a low computational cost, and is explicitly based on the higher-order structure in the spiking patterns. We then applied SpikeShip to large-scale Neuropixel recordings during spontaneous activity and visual encoding. Using SpikeShip, we show that high-dimensional spiking sequences reliably distinguish between different natural images and different behavioral states. These spiking sequences carried complementary information to conventional firing rate codes. SpikeShip opens new avenues for studying neural coding and memory consolidation by finding patterns in high-dimensional neural ensembles.

Introduction

Information in the brain is encoded by very high-dimensional "ensembles" of neurons, which encode information by firing nerve impulses ("spikes"). Populations of neurons can produce specific spike patterns depending on sensory inputs or internal variables [1–8]. With new recording techniques like Neuropixels [9], it has become possible to simultaneously record from thousands of single neurons [10–12]. This offers new opportunities to uncover the relationship between multi-neuron spiking patterns and sensory inputs or motor outputs, yet also poses unique mathematical challenges for the unsupervised discovery of the "dictionary" of neuronal "code-words". For instance, how do we measure the similarity between two multi-neuron spiking patterns in terms of their temporal structure (spike sequence)?

In general, the notion of information encoding relies on the construction of a distance or dissimilarity measure in an N-dimensional space. For example, the distance between binary strings can be measured using the Hamming distance, an essential mathematical construct in error-correcting coding. In the brain, the distance between two multi-neuron spiking patterns is conventionally measured in two steps: (1) By computing the number of spikes/sec (firing rates) for each neuron in a certain time window; and (2) computing e.g. the angle or Euclidean distance between multi-neuron rate vectors. Using this method, it has been shown for example that high-dimensional neural ensembles span a low-dimensional manifold that relates to stimulus or behavioral variables in a meaningful way [13, 14]. However, firing rates do not capture the potentially rich information contained by the precise temporal order in which spikes are fired, e.g. neuron i firing at time t and neuron j firing at $t + \tau$. For instance, we expect that any time-varying sensory stimulus or action sequence may be encoded by a unique multi-neuron temporal pattern of spiking. Indeed, multi-neuron temporal sequences can encode information about sensory stimuli and are required for the generation of complex motor patterns like bird songs [1–7, 15, 16]. Temporal sequences may also be critical for memory formation, because neural plasticity rules are highly sensitive to the temporal order in which spikes are fired [17–21].

Previously, we have developed a dissimilarity measure between multi-neuron temporal spiking patterns called SPOTDis (Spike Pattern Optimal Transport Dissimilarity). SPOTDis was defined as the minimum energy (optimal transport) that is needed to transform all pairwise cross-correlations of one epoch k into the pairwise cross-correlations of another epoch m. We showed that, due to employment of optimal transport, SPOTDis has several attractive features (see Results) [22], and can be combined with unsupervised dimensionality-reduction and clustering techniques to the state-space of multi-neuron temporal sequences. However, SPOTDis has two principal weaknesses that we address here: (1) Its computational complexity, for comparing two time epochs, is $\mathcal{O}(N^2)$, where N is the number of neurons. This becomes a major problem for computing an $M \times M$ dissimilarity matrix (for M time epochs) for thousands of neurons. (2) It relies exclusively on pairwise spike-timing relationships (i.e 2nd order correlations), because it does not solve the optimal transport problem for the entire spike pattern, but only for neuron pairs separately. Hence, it may not be sensitive to higher-order correlations in spiking patterns.

Here, we develop a novel dissimilarity measure for multi-neuron spiking patterns called SpikeShip, which has linear computational complexity of $\mathcal{O}(N)$. We achieve this by (1) computing the minimum transport cost of spikes for each spike train separately, and (2) discounting a global translation term in the transport flow across neurons. SpikeShip can be interpreted as the optimal transport cost to make all spike-timing relationships between two different multi-neuron spiking patterns identical. That is, it solves the optimal transport problem for the entire spiking pattern and is thus sensitive to the higher-order structure of spike trains. We demonstrated the power of the SpikeShip measure by applying it to large scale, high-dimensional neural ensembles in mice from [12] and [23]. Using SpikeShip, we show that temporal spiking sequences reliably distinguish between natural stimuli and different brain states.

Results

Our overall goal is to develop a dissimilarity measure between multi-neuron spiking patterns that is exclusively based on the temporal order of spiking (i.e. not on the spike count). Suppose that we have measured the spikes from N neurons ("spike trains"). Spike trains are divided into M epochs of length T (measured in seconds or samples). Epochs could be defined by e.g. trials (e.g. stimulus presentations) or sliding windows [22]. The

problem is to find a dissimilarity measure with the following properties [22]:

1. The measure should depend on the temporal order of firing across neurons, but not on the spike count, although the dissimilarity measure below can be generalized to incorporate spike count differences.

2. If two spike patterns are identical in terms of cross-neuron spike timing relationships (i.e. temporally translated version of one another), then the dissimilarity measure should equal zero.

3. The measure does not require binning or smoothing, and is based on the exact timing of the spikes.

4. It should allow for the discovery of more patterns than the number of neurons, when used in combination with clustering techniques like HDBSCAN.

5. It should measure dissimilarity in a continuous way and avoid the problem of "combinatorial explosion". This problem occurs with methods that search for exact matches in spiking patterns, if the number of neurons is large.

Previous work: SPOTDis

[22] developed a dissimilarity measure called SPOTDis, which is based on optimal transport theory. We briefly summarize the computing steps of SPOTDis (see Methods):

1. Compute cross-correlation histograms for all N^2 pairs (i, j) of two neurons, $s_{ij}^{\text{norm}}(k)$. These cross-correlations capture the information about the spike-timing relationships across all pairs of neurons.

2. Normalize these histograms to unit mass, which is needed for the optimal transport measure, and removes the effect of spike count.

3. Compute, for each pair of neurons (i, j) and pair of epochs (m, k), the minimum transport cost (Earth Mover's Distance) to transform $s_{ij,k}^{\text{norm}}$ into $s_{ij,m}^{\text{norm}}$. This yields a dissimilarity measure denoted $D_{ij,km}$.

4. Compute the average of this dissimilarity measure across all pairs of neurons, yielding a dissimilarity measure D_{km} called SPOTDis.

Using simulations, we showed that SPOTDis can be used to find distinct clusters of multi-neuron spiking patterns in an unsupervised way [22].

As discussed in [22], SPOTDis satisfies the six requirements listed above. In particular, note that the EMD can be computed based on exact spike times and does not require binning or smoothing.The use of the EMD for multi-neuron spike train dissimilarity has several additional advantages, as explained in [22]: The EMD is a symmetric and metric measure of similarity between two probability distributions (unlike the KL-divergence). In contrast to KL divergence, it does not quantify whether two distributions are overlapping in *the same bins*; rather, it examines how far distributions are shifted away from each *across bins* in a metric space (in this case: time). Different from KL, EMD is well behaved both when comparing continuous and discrete (sum of delta functions) distributions. Further, the EMD does not rely on the computation of a measure like the center of mass or the peak time of firing activation, but can deal with multi-modal spiking patterns.In other words it does not require any prior specification of features. Finally, as shown in [22], SPOTDis is highly noise robust (i.e. to insertion of noise spikes or spike-time jitter) because of the use of EMD.

SpikeShip

There are two main problems with the construction of SPOTDis: First, its computational complexity scales as $\mathcal{O}((Nn)^2)$, where n is the average number of spikes per epoch. Note that this computation typically needs to be carried out M^2 times in order to create a dissimilarity matrix for all epoch-to-epoch comparisons. This means that in practice, computation of SPOTDis might not be feasible when N is on the order of thousands, which is nowadays achievable with modern recording technologies. Second, as discussed in [22], SPOTDis is based exclusively on the pairwise cross-correlations between neurons. Hence, it may be insensitive to the higher-order correlations in the spike trains.

To address these problems we introduce the SpikeShip measure (see Methods). SpikeShip yields a dissimilarity between multi-neuron spike train patterns that has similar characteristics as SPOTDis. But, it is has the following desirable properties:

1. Its computational complexity grows linearly with the number of neurons and spikes, i.e. $\mathcal{O}(Nn)$.
2. By construction, it is sensitive to higher-order spike-timing relationships.
3. It allows for the decomposition of transport cost into a temporal rigid translation term and neuron-specific flow terms.

SpikeShip is computed in two steps (see Methods, Fig. 1):

1. Compute the optimal transport flow to transform a spiking pattern in epoch k into the spiking pattern in epoch m. This flow vectors are computed for each neuron separately (i.e. in the spike raster plot, mass from spikes can be moved horizontally, but not vertically). This is performed in two steps: (i) Assign a mass to each spike, such that the total mass for the ith neuron in epoch k and m is equal; (ii) compute for each spike, how its mass should be shifted in order to make the spike trains in the window T completely identical.
2. By using an expression for a global temporal translation term (across neurons) and subtracting this from all the spike shifts, we minimize the overall transport cost. This transport cost amounts to the amount of energy to shift the individual spikes such that all spike-timing relationships across neurons become identical.

When we compute the EMD in step 1, we can compute the total transport in discrete steps, shifting mass from a spike in pattern k to mass of a spike in pattern m. This can be algorithmically solved, for each neuron, in approximately order $\mathcal{O}(n)$. We denote the discrete steps $c_{i,u}$ with moved mass $w_{i,u}$, such that $\sum_u w_{i,u} = 1$. From these flows computed in Step 1, we can then subtract a global rigid translation term. This uniquely yields the minimum transport cost to transform the multi-neuron spiking pattern in epoch k such that its spike-timing relationships are identical to another pattern m. In the Methods section we state our main result, namely that the optimal transport flows are given by

$$f_{i,u} = c_{i,u} - g^{\min} \,. \tag{1}$$

Here $g^{\min}$ is the weighted median across all the original flows $c_{i,u}$ with associated mass $w_{i,u}$. Thus we can decompose the transport flow in two terms: (1) an optimal global shift between two epochs, shared across all neurons; and (2) an optimal neuron-specific transport flow based on the EMD method. We then define SpikeShip (see Methods) as

$$F_{km} \equiv \frac{1}{|\mathcal{A}_{km}|} \sum_{i \in \mathcal{A}_{km}} w_{i,u} \sum_{u=1}^{n_i^*} |f_{i,u}| \,. \tag{2}$$

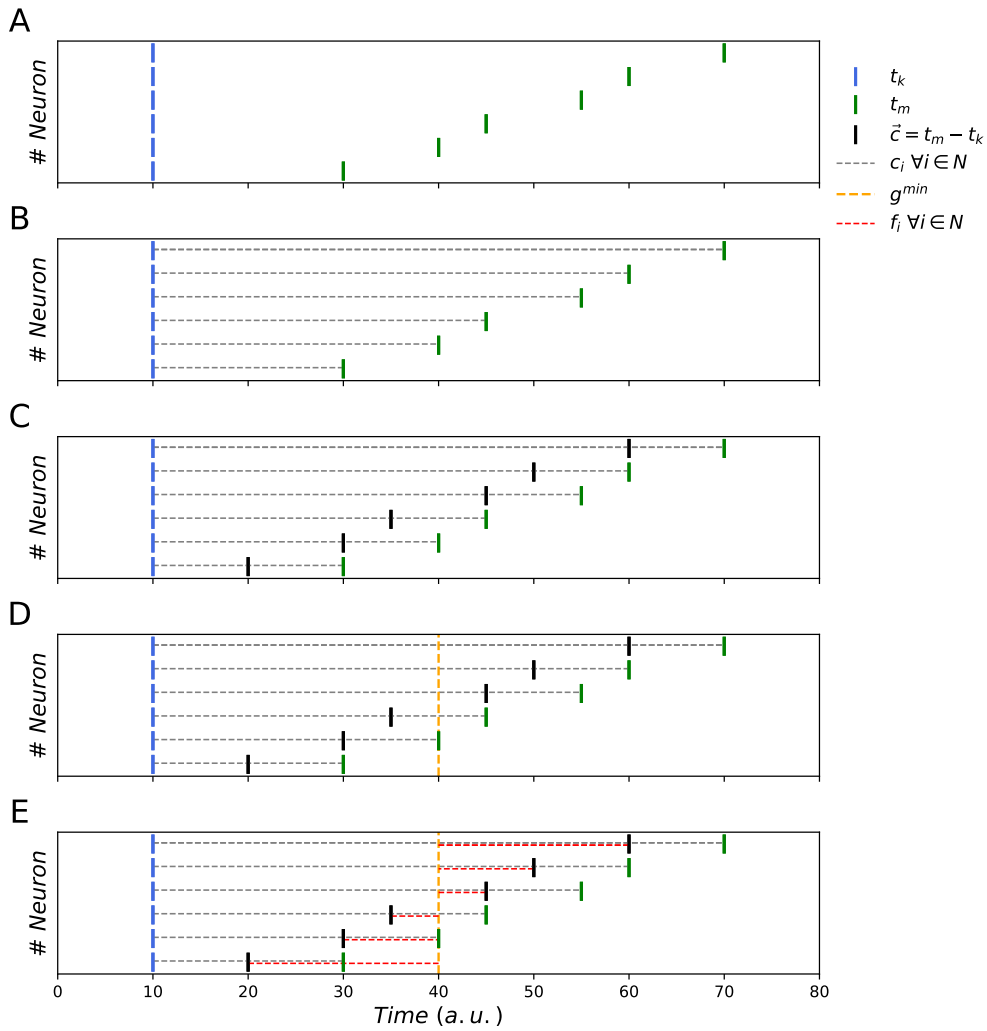

Fig 1. Illustration of SpikeShip A) Example of two epochs with spike times $t_k = (10, 10, 10, 10, 10, 10)$ and $t_m = (20, 30, 35, 45, 50, 60)$ (note only one spike per neuron in this example). B) Distances between spike times t_k and t_m. C) The vector $\vec{c}$ contains the differences of spike times t_k and t_m. D) Computation of the median of $\vec{c}$: $g^{\min} = 30$. E) $g^{\min}$ is the optimal global shift such that $f_i = c_i - g^{\min}$. The neuron-specific shifts $\vec{f} = (-20, -10, -5, 5, 10, 20)$ contain all the information about the structure of distances between t_k and t_m. SpikeShip equals $F_{km} = \frac{1}{6}\sum_i^N |f_i| = \frac{70}{6}$.

Here $\mathcal{A}_{km}$ is the set of all neurons that fired a spike both in epoch k and m. The weight $w_{i,u} = \frac{1}{n_i^*}$, effectively assigns an equal weight to each neuron that contains at least one spike. The algorithm to compute SpikeShip has computational complexity $\mathcal{O}(Nn)$, because the weighted median has complexity $\mathcal{O}(N)$ (Fig. 2). This result is, in a way, surprising: One would expect that for a dissimilarity measure that is based on the relative spike-timing between neurons and is sensitive to higher-order correlations, we would need a computational complexity of at least $\mathcal{O}(N^2)$.

Relationship between SpikeShip and SPOTDis

We show in the Methods section that there exists an analytical relationship between SpikeShip and SPOTDis for a specific class of sequences: Suppose that (1) in each temporal sequence, a neuron is active in only in a small part of the time window T (or fires only one spike), and (2) that the temporal sequence is uniformly spanned across neurons (i.e. a uniform distribution across neurons). The relationship between SPOTDis and SpikeShip (see Fig. 2) then equals

$$D_{km} \approx \frac{7}{5} F_{km} \,. \tag{3}$$

Thus, for these kind of sequences, the total transport cost F_{km}, which equalizes all the higher-order correlations in the spike patterns, can be related to the transport cost over all the pairwise spike-timing relationships (SPOTDis). However, an analytical relationship may not exist for the case of multimodal spiking patterns or other types of distributions (see e.g. Example 1).

SpikeShip is a more sensible dissimilarity measure than SPOTDis because it is explicitly sensitive to higher-order structure in the spike train. In addition, it is $\mathcal{O}(Nn)$ faster. The difference between SpikeShip and SPOTDis can be further illustrated with the following simple examples.

Example 1: Suppose that we have a pair of vectors of spike times $\vec{t}_k = (0, 0, 0, 0)$ and $\vec{t}_m = (-20, 0, 0, +20)$. We now have cost $\vec{f} \equiv (-20, 0, 0, +20)$ and $F_{km} = \frac{40}{4} = 10$. The SPOTDis in this case equals

$$\frac{2 \times (0 + 20 + 20 + 40) + 2 \times (0 + 0 + 20 + 20)}{16} = 15 \,. \tag{4}$$

Consider now another vector of spike times $\vec{t}_k = (0, 0, 0, 0)$ and $\vec{t}_m = (-15, -15, +15, +15)$. We now have cost $\vec{f} \equiv (-15, -15, +15, +15)$ and, different from above, $F_{km} = \frac{60}{4} = 15$. The SPOTDis in this case equals

$$\frac{4 \times (0 + 0 + 30 + 30)}{16} = 15 \,, \tag{5}$$

In this case, the mover costs on the 2nd order pairwise timing relationships (SPOTDis) are the same for both pairs of sequences; however, SpikeShip correctly reflects the increased mover cost that is needed to match the two patterns to the zero pattern. We can consider further the SpikeShip dissimilarity between the two sequences $(-15, -15, +15, +15)$ and $(-20, 0, 0, +20)$ (1st and 3rd sequence in Fig. 2E). In this case, SpikeShip equals $F_{km} = \frac{40}{4} = 10$. However, SPOTDis now equals $D_{km} = \frac{280}{16} = 17.5$. Thus, SPOTDis assigns a disproportionally large transport cost between the two sequences as compared to the $(0, 0, 0, 0)$ sequence (Fig. 2E).

Dissimilarity matrix and cluster visualization

We compute SpikeShip to detect unique, recurring spiking patterns generated as in [22] (Fig. 3). The dataset contains $P = 7$ patterns across $N = 100$ neurons and $M = 360$

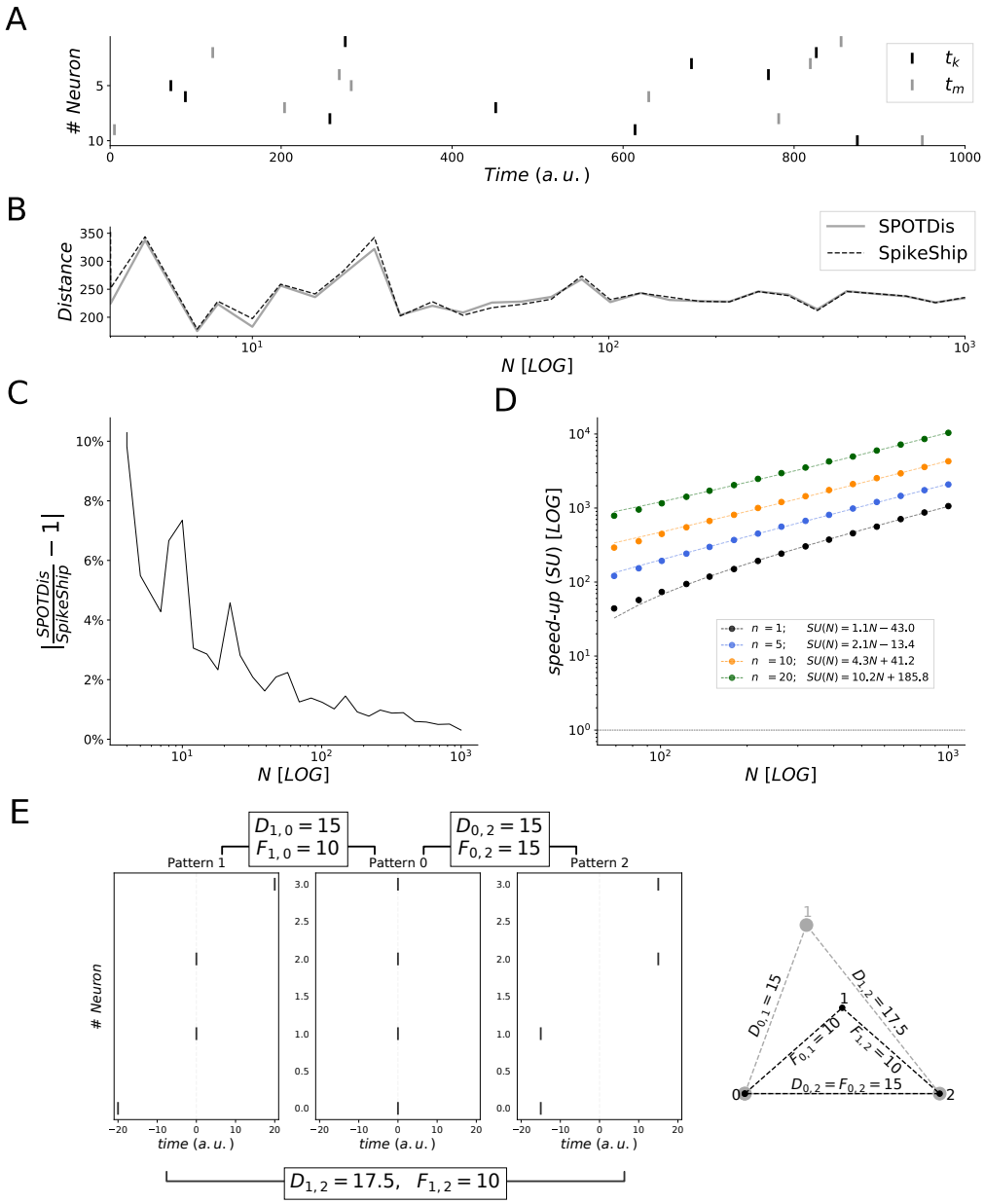

Fig 2. Accuracy and Speed-up comparison for single- and multi-spike patterns. A) Example of single spike trains for two epochs for 10 neurons. Patterns were generated as uniform sequences with 1 spike per neuron per epoch. B) Values of SPOTDis and SpikeShip as a function of the number of neurons N. The value of SpikeShip is scaled by a factor $\frac{7}{5}$ based on the analytical relationship for patterns with a single spike per neuron. Note that this simulation confirms the analytical relationship between SPOTDis and SpikeShip (see Methods). C) Difference between SpikeShip vs. SPOTDis (scaled by same factor as in (B)) expressed as percentage. D) Computational speed-up (log-scale) for SpikeShip vs. SPOTDis (serial execution) for increasing amount of neurons N. Speed-up is approximately N when there is 1 spike per neuron, and it increases when $n > 1$ (i.e. the multi-spike pattern case). E) Example of three single-spike patterns: $(-20, 0, 0, +20)$, $(0, 0, 0, 0)$, and $(-15, -15, +15, +15)$, from left to right. SpikeShip assigns a geometrically more appropriate transport cost between pattern 1 and 2 ($F_{1,2} = 10$) than SPOTDis ($D_{1,2} = 17.5$), considering their distance with pattern 0.

epochs. Low-dimensional embedding was performed with t-SNE [24, 25] as in [22] (Fig 3B). Clusters were derived using HDBSCAN [26] and are plotted in a 2-dimensional space. These matrices were computed using a workstation with 12 CPU cores (DUAL Xeon E5646 @ 2.40GHz). The computation time for SpikeShip and SPOTDis dissimilarity matrices were 28.2 sec and 20186.2 secs (5 hours, 36 minutes, and 26.2 secs), respectively. This is a speedup of about 700 times (which is higher than $N = 100$ due to presence of multiple spikes).

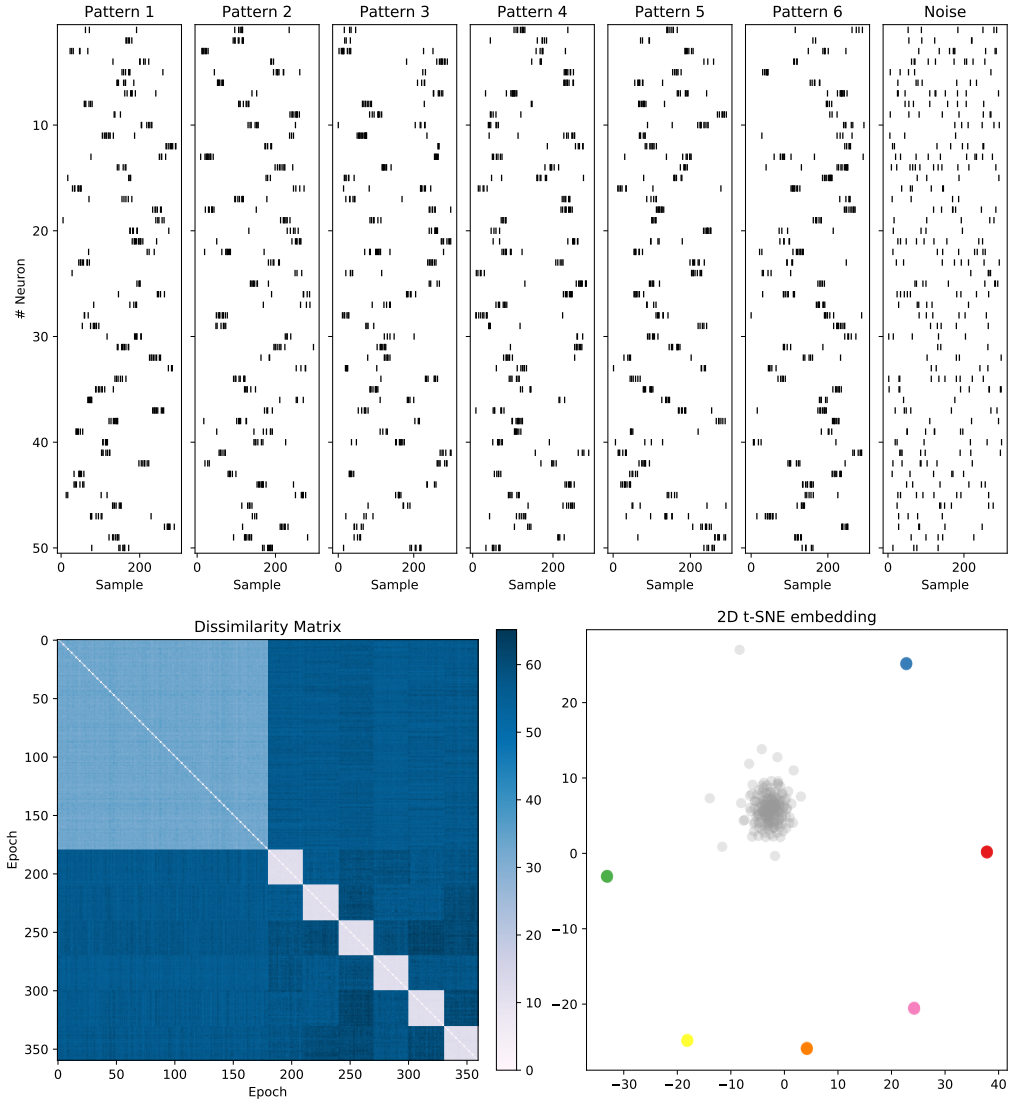

Fig 3. Dissimimilarity matrices and clustering comparison. Top: Samples from simulated neuronal outputs according to an inhomogenous Poisson process (using scripts provided by [22]). Bottom: Sorted Dissimilarity matrix by pattern using SpikeShip dissimilarity measures (left), and a 2-dimensional t-SNE embedding using SpikeShip dissimilarity matrix (right).

Application to Allen Brain Institute's neural datasets

Next, we applied SpikeShip to several high-dimensional neural datasets. Previous work has shown that the visual system can very rapidly process natural images and extract categorical information [27]. It has been proposed that this relies on a temporal coding strategy, whereby visual information is encoded based on the temporal sequence of spikes relative to stimulus onset [27].

Here, we used SpikeShip to determine whether temporal spiking sequences in area V1 can reliably distinguish natural images from each other. To this end, we analyzed Neuropixel data from 32 mice while they passively viewed natural images (dataset from the Allen Institute for Brain Science; see Methods). A total of 20 natural scenes were selected with 10 repetitions each (i.e. $M = 200$ epochs) as shown in Fig. 4A. To create a high-dimensional vector of neurons, we pooled together all recorded neurons ($N = 8,301$) across the 32 mice (See Fig. 4B). Because these neurons were recorded in different sessions, only evoked spiking sequences that were time locked to stimulus onset were preserved in the data. The computation time for SpikeShip to compute one dissimilarity matrix of Fig. 4C was on average 58.8 secs (see Methods), thus indicating a highly effective computation time for $N = 8,301$ neurons. In contrast, we estimate the computation time for the previous SPOTDis measure to be approximately 175.71 hours (based on $n \approx 3.33$ spikes per neuron).

The pairwise SpikeShip distance is presented in Fig. 4C as a dissimilarity matrix sorted by the presentations of each natural scene. The t-SNE embedding revealed clear clustering of spiking patterns based on SpikeShip, such that different natural images could be reliably distinguished from each other (See Fig. 4D). Hence, natural images yielded distinct temporal spiking sequences that were time-locked to stimulus onset, in support of the idea that the visual system may use a temporal coding strategy.

Comparison of SpikeShip vs firing rates in visual stimuli

We wondered how the information in temporal spiking sequences compared to the information carried by conventional firing rate codes. Our first question was, which one of these two codes conveyed more information. To determine this, we computed a distance matrix for the firing rates, by computing the Euclidean distance between the firing rate vectors. These distances were computed in the same time window as we used for SpikeShip (Fig. 5A). We then computed a measure of discriminability between natural images based on the distances within and between images (see Methods 36).

We found that there was a higher discriminability between natural images for SpikeShip as compared to firing rate vectors for all the natural scenes (Fig. 5B). Correspondingly, the t-SNE visualization yielded a clearer definition of clusters in the low-dimensional space (Fig. 5C).

Next, we wondered to what extent the information in SpikeShip was independent of the firing rate information. To this end, we computed the Spearman correlation between the SpikeShip distance and firing rate dissimilarity matrices, which contained information from all epochs across all natural images. We found that the dissimilarity matrices of SpikeShip and firing rates were only weakly correlated across epochs (Spearman correlation equals 0.1804). Accordingly, the t-SNE visualization shows that the relative locations of the clusters show major differences between both methods (Fig. S7).

Altogether, these results show that SpikeShip and firing rates contain different and to a large extent independent information about natural stimuli. Furthermore, SpikeShip allowed for a better separation of the different natural stimuli in comparison to firing rates. These findings supports the idea that the visual system may use spiking sequences to encode information about natural scenes, as proposed by [27].

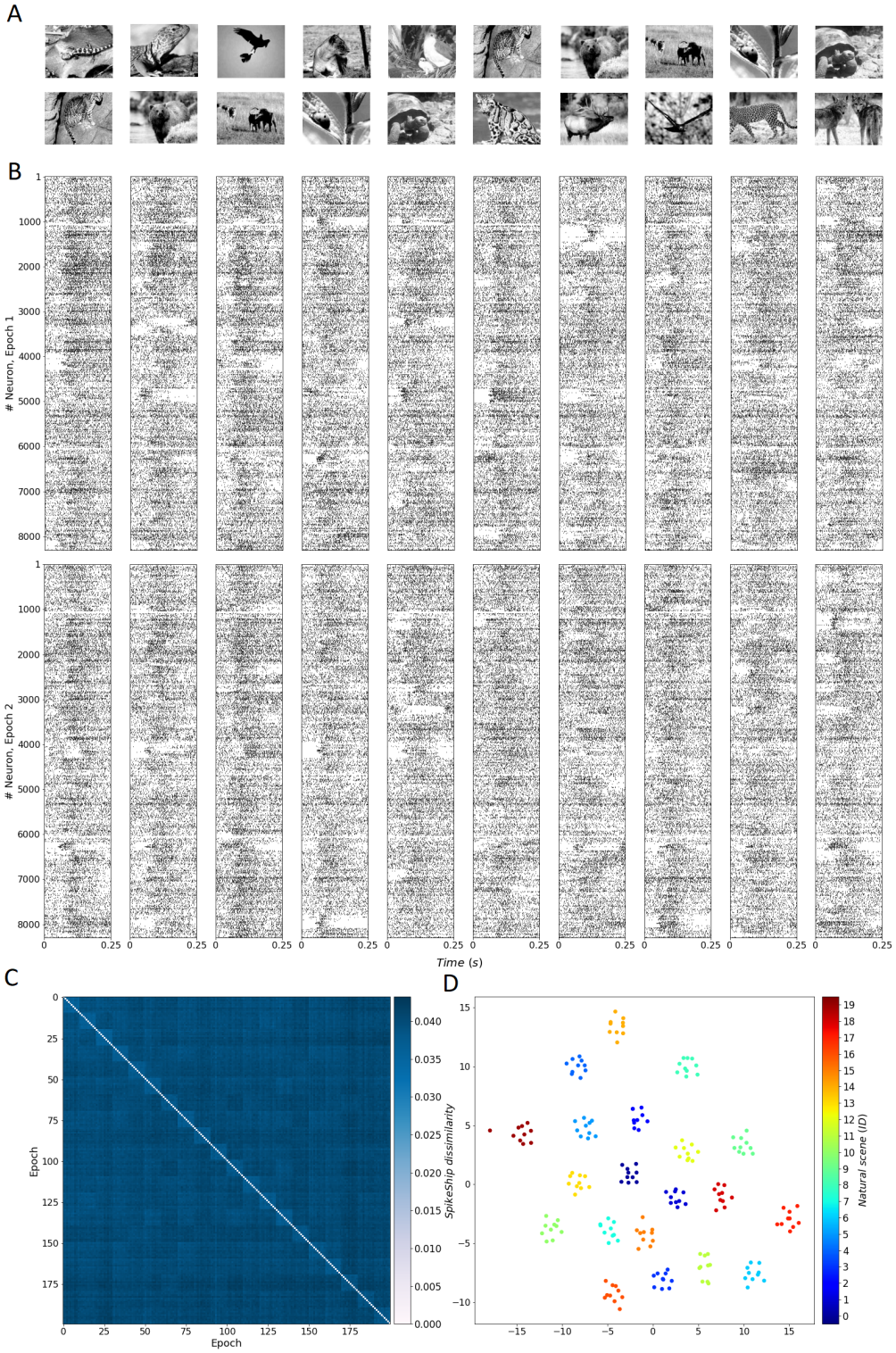

Fig 4. SpikeShip analyzis of spike sequences for natural scenes presentations (Allen Brain Institute). A) Sample of 20 Natural Scenes from Allen Brain Institute's dataset. B) Raster plot of two epochs with $N = 8,301$ neurons for each presentation. C) Left: Sorted dissimilarity matrix by image ID for 20 natural scenes presentations with 10 presentations each ($M = 200$). Right: 2-dimensional t-SNE embedding for each presentation.

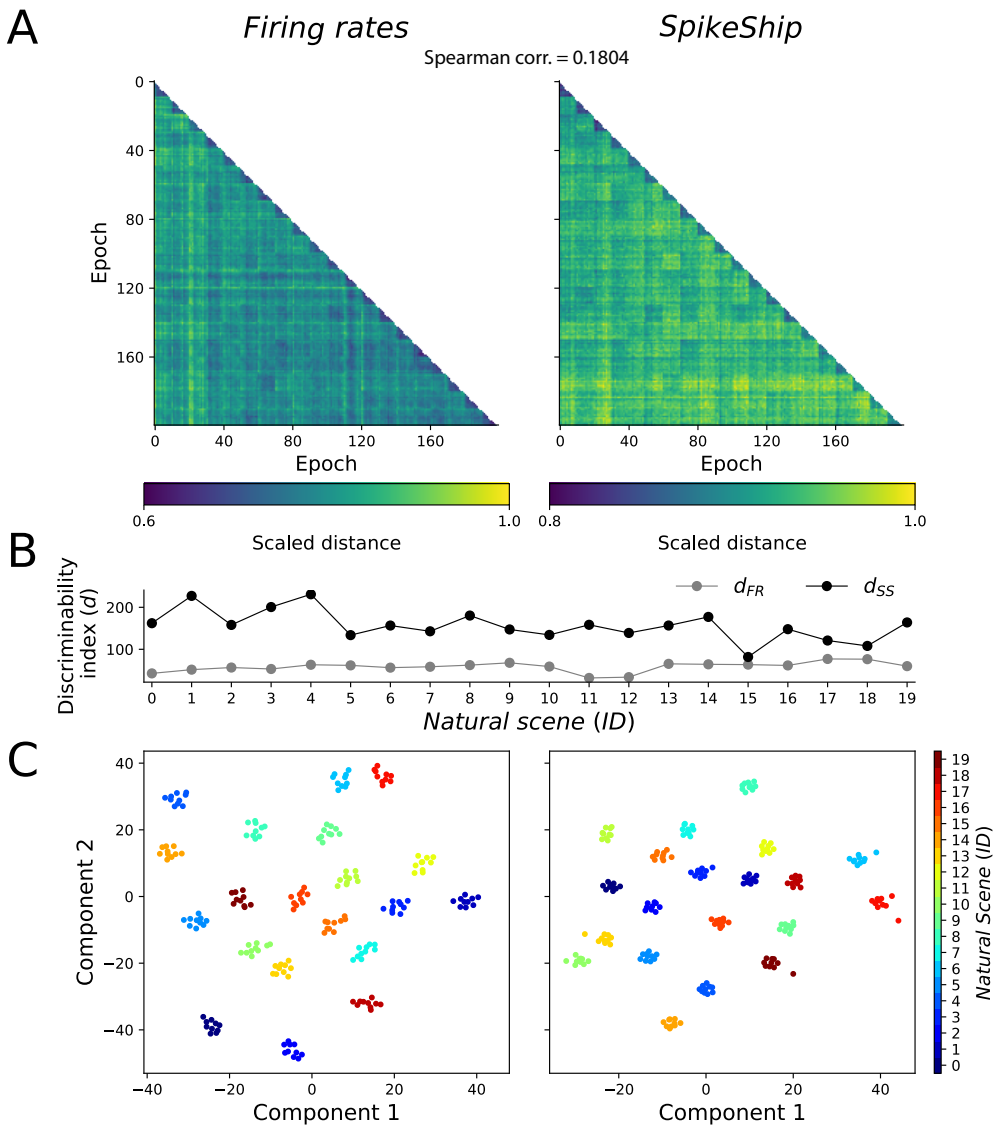

Fig 5. Comparison of pairwise distances between Firing rates and SpikeShip. A) Dissimilarity matrices for Allen Brain Institute data (sorted by natural scenes). Colormaps were changed to show more variability in distances. B) Discriminability index for dissimilarity matrices shown in A) by using firing rates (d_{FR}) and SpikeShip (d_{SS}). C) 2D t-SNE embeddings for dissimilarity matrices shown in A) for firing rates (left) and SpikeShip (right).

Application to spontaneous activity

Next, we applied SpikeShip to high-dimensional neural recordings from multiple brain areas while mice spontaneously transitioned between different behavioral states. Previous work has shown that behavioral states have major effects on the firing rates of neurons across multiple brain areas [10, 28]. Recent work has shown that different facial motion components outperform the prediction of firing rates as compared to running speed and pupil diameter (a measure of arousal). Hence, we wondered whether different behavioral states are accompanied and distinguished by specific spiking sequences.

To investigate this, we analyzed the data set of [23], which contains multi-areal recordings from > 1000 neurons in three mice. Similar to [10], we distinguished between different states based on the facial motion components using the SVD (singular value decomposition), and identified low, medium and high-motion epochs (Figure 6A-C). We randomly selected one hundred epochs for both low-, medium and high-motion states and computed the SpikeShip dissimilarity matrix ($M = 200$, See 6D). For these experiments, SpikeShip took 25.5 secs in creating a dissimilarity matrix. Considering $N \approx 2,500$, $n \approx 5$, based on Fig. 6D, the computation time of SPOTDis can be estimated as as 34.06 hours (1 day and 10.06 hours; $SU \approx 4,808$).

In Fig. 6E, we show the dissimilarity matrix for one mouse ("Waksman"; $N = 2,688$, for the other two mice see Fig. S8). The first 100 epochs represent low-motion states, and the remaining 100 are the middle- and high-motion epochs. The dissimilarity matrix reveals that the spiking sequences during medium and high motion are relatively similar to each other, whereas there is a relatively high variability among sequences during low-motion epochs (Fig. 6E-F). Furthermore, both the t-SNE embedding and the spectral embedding show a separate state-space region for the spiking sequences during medium and high motion.

We further wondered if SpikeShip contains orthogonal information compared to firing rates, similar to what we had observed for natural images. Again, we computed the Spearman correlations between the SpikeShip and the firing rate dissimilarity matrices. We found relatively weak correlations between the firing rate and SpikeShip dissimilarity matrices for the three mice: $(0.189, 0.024, -0.064)$ for $N = (1462, 2296, 2688)$ neurons, respectively (See Fig. 6. We found relatively weak correlations between the firing rate and SpikeShip dissimilarity matrices for the three mice: $(0.189, 0.024, -0.064)$ for $N = (1462, 2296, 2688)$ neurons, respectively (See Fig.

We found relatively weak correlations between the firing rate and SpikeShip dissimilarity matrices for the three mice: $(0.189, 0.024, -0.064)$ for $N = (1462, 2296, 2688)$ neurons, respectively (See Fig. 6G).

G). These findings further support the notion that spiking sequences and firing rates may convey relatively independent information.

Altogether, these findings indicate that different brain states give rise to specific temporal correlation patterns across neurons, with relatively homogeneous spiking sequences during active behavior as compared to quiescence.

Discussion

We studied the problem of measuring the dissimilarity between two multi-neuron spiking patterns based on the relative spike-timing relationships across neurons (i.e. firing order). We developed a new measure called *SpikeShip*. SpikeShip solves the problem of optimally transporting the spikes of individual neurons, such that the global pattern of spike-timing relationships becomes identical between two epochs. Intuitively, one would think that such a measure has computational complexity of at least $\mathcal{O}(N^2)$, but we show that it can be computed with $\mathcal{O}(N)$ computational complexity; this is a major improvement

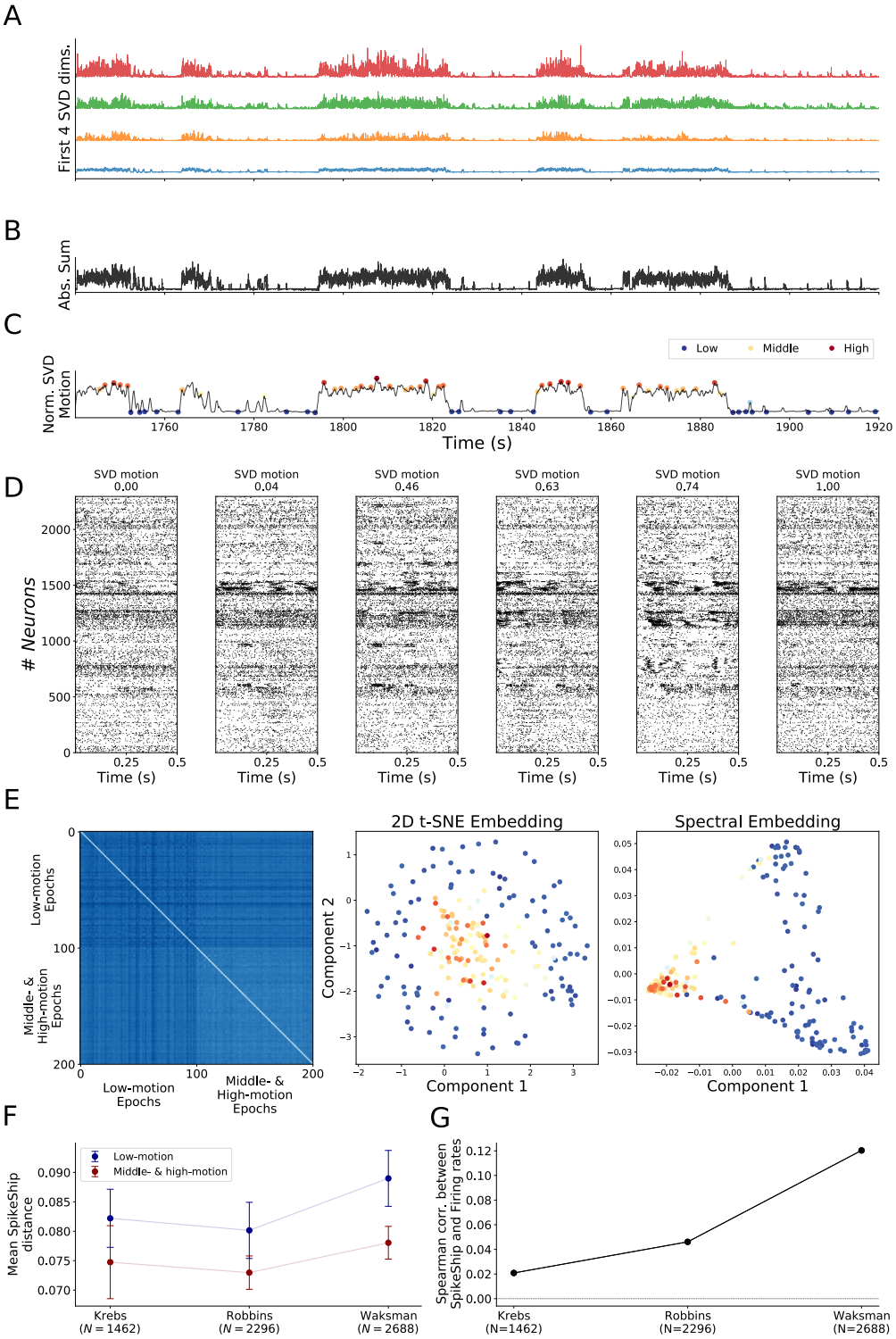

Fig 6. Spontaneous activity analyzes. A) First 4 SVD dimensions of [23] dataset. B) subtraction of the median of the first four SVD motion dimensions (denoising). C) Normalized SVD motion used to detect low- and high-states. Circles represent samples of temporal windows for posterior analyzes. D) Raster plot for $N = 2,296$ neurons for different epochs. E) Multi-spike sequence analyzes. Left: Dissimilarity Matrices. Middle: 2D t-SNE embedding. Right: 2D Spectral Embedding (Laplacian Eigenmaps). F) Mean SpikeShip distance from [10] experiments. G) Spearman correlation between firing rates and SpikeShip per experiment.

over our previous work [22]. We show that a dissimilarity between two spiking patterns can be decomposed into neuron-specific flows and a temporal rigid translation term. Compared to our previous measure SPOTDis [22], SpikeShip is not restricted to the 2nd order correlations, but is based higher-order structure in the spike train.

Our technique can also be used to align temporal sequences in an unsupervised way if there is a global jitter between spike patterns. This achieves a similar goal as a recent study [29], described as "warping"; however, the method in our paper does not require any parameter estimation; furthermore, it can also be used to align trials corresponding to different stimuli or behavioral conditions. For example, suppose that we want to analyze the sequence of neural activation in relationship to some event, e.g. freely moving your arm. Suppose that we do not know the exact onset of the neuronal sequence in relationship to moving your arm, and we record multiple realizations of this event. With SpikeShip, we can immediately decompose the transport cost between any two trials in terms of a global translation term (which is a non-linear computation) and a neuron-specific shift. This allows one to align trials that were recorded in different conditions, e.g. moving your arm left or right. And it yields, in essence, a state-space characterization of temporal trajectories (e.g. related to different movements), rather than a trajectory through a state-space of firing rate vectors.

We applied SpikeShip to large, real neuronal datasets of experiments in mice. We found that SpikeShip can be used for the unsupervised decoding of different natural images from a high-dimensional temporal spiking pattern across > 8000 neurons. Interestingly, we found that SpikeShip outperformed the classical firing rate vector, and that the spike timing information was only weakly redundant with the information in the firing rate vector. This suggests that spike timing information carries additional information relative to the firing rate, as has been hypothesized by [27]. Such a spike timing code could subserve the rapid feed-forward transmission of information to higher brain areas based only on the timing of the first spikes. It is known that feed-forward transmission of information depends strongly on the initial bout of activation in which neurons may fire only a few spikes [30]. Interestingly, the SpikeShip technique does not require the explicit identifications of spike latencies, and is able to extract higher-order correlations from spiking patterns and also distinguish multimodal patterns from each other [22]. Furthermore, as we showed here, the computation is extremely efficient. We further analyzed large-scale recordings from visual cortex, retrosplenial, sensorimotor, frontal, striatum, hippocampus, thalamus, and midbrain. We showed that the temporal structure of spike train distinguished between low- and high-motion epochs, and again provided orthogonal information to the firing rate code. Furthermore, we found that spiking patterns become more homogeneous during high-motion epochs, which is consistent with the notion that arousal improves the reliability of signal transmission in the cortex [28].

SpikeShip opens new avenues to study temporal sequences in high-dimensional neural ensembles. Recent technological developments now allow for recordings of thousands of neurons simultaneously, either using electrical recordings or two-photon imaging [9]. The technique developed here is applicable to both kinds of data, due to linear computation time. Application of SpikeShip to such kind of data might generate important insights into the role of temporal sequences in sensory coding and memory consolidation.

Materials and methods

Previous work: SPOTDis

We previously defined a dissimilarity measure between multi-neuron spike train patterns called SPOTDis [22]. We give a brief overview of the definition of the SPOTDis measure; for a detailed account we refer to [22]. Suppose we record spike trains of N neurons in M

separate epochs (e.g. trials); we refer to these as "spike patterns". SPOTDis was defined as follows: We first compute, for all M epochs separately, a normalized cross-correlation function for all N^2 pairs of neurons,

$$s_{ij,k}^{\text{norm}}(\tau) \equiv \frac{s_{ij,k}(\tau)}{\sum_{\tau=-T}^{T} s_{ij,k}(\tau)}\,, \tag{6}$$

where $s_{ij,k}(\tau) \equiv \sum_{\tau=-T}^{T} s_{i,k}(t)s_{j,k}(t+\tau)$ is the cross-correlation function (or cross-covariance), and $s_{i,k}(t)$ and $s_{j,k}(t)$ are the spike trains of neurons i and j in the kth trial. The normalization of the cross-correlation function is necessary to avoid an influence of firing rate fluctuations, and to compute the EMD. Next, we compute the Earth Mover Distance (EMD) between the normalized cross-correlograms $s_{ij,k}^{\text{norm}}(\tau)$ and $s_{ij,m}^{\text{norm}}(\tau)$ for each (k,m). This yields $M(M-1)/2 \times N(N-1)/2$ EMD values $D_{ij,km}$. In [22], we used the L1 norm to measure dissimilarity on the time axis, but the L2 norm could be used as well. After computing the EMDs between each pair of epochs for each neuron pair separately, we compute SPOTDis as the average EMD across neuron pairs,

$$\bar{D}_{km} \equiv \frac{1}{|\mathcal{A}_{km}|} \sum_{(i,j)\in\mathcal{A}_{km}}^{N} D_{ij,km}\,. \tag{7}$$

Here, $\mathcal{A}_{km} \equiv \{(i,j) : n_{i,m} > 0 \wedge n_{i,k} > 0 \wedge n_{j,m} > 0 \wedge n_{j,k} > 0\}$, i.e. the set of all pairs of neurons that are active in both epochs k and m. We ignored the other neuron pairs (i.e. not contained in this set) for computing the SPOTDis, because it avoids assigning an arbitrary value to the EMD when there is no information about the temporal relationship between the neurons (i.e. when we do not have any spikes for one neuron in one epoch).

Derivation of SpikeShip

A major problem with the computation of SPOTDis (for all pairs of epochs) is that it has computational complexity of $\mathcal{O}(N^2M^2)$. Furthermore, because it is based on 2nd order correlations, it is not explicitly sensitive to higher-order correlations. Here we derive a new dissimilarity measure, called SpikeShip, which has computational complexity $\mathcal{O}(N)$ for one pair of epochs. To derive this measure, we first consider the simplified case where each ith neuron fires one spike for all M epochs.

SpikeShip for a single spike per epoch

Let $\vec{f}_{km} = (f_{1,km}, \ldots, f_{N,km})$ be a vector of flows for each neuron in epoch m. In other words, $f_{1,km}$ is the shift of the spike fired by the first neuron in the mth epoch. The total moving cost equals

$$F_{km} \equiv \frac{1}{N}\sum_{i=1}^{N} |f_{i,km}|\,. \tag{8}$$

The problem statement is to find a flow vector $\vec{f}_{km}$ such that after moving the spikes, the resulting spike train patterns are identical between epoch k and epoch m, in terms of the full matrix of spike timing relationships. We wish to find the flow vector that satisfies this constraint with minimum cost F_{km}.

Example: Consider the following example: Suppose there are two epochs for $N = 6$ neurons with spike times $\vec{t}_k = (10, 10, 10, 10, 10, 10)$ and $\vec{t}_m = (20, 30, 35, 45, 50, 60)$. We will show that the flow vector with minimum cost, such that spike patterns have identical temporal structure, equals $\vec{f}_{km} = (-20, -10, -5, 5, 10, 20)$ (Fig. 1).

More formally, let $t_{m,i}$ be the timing of the spike for the ith neuron in the mth epoch. We denote the spike times after (post) moving them in epoch m as

$$t_{m,i}^{\text{post}} \equiv t_{m,i} - f_i \tag{9}$$

$\forall i$, where we omitted the subscripts k, m from the variable $f_{i,km}$ for simplicity. The constraint that all the across-neuron spike timing relationships should be identical after moving implies that

$$t_{m,i}^{\text{post}} - t_{m,j}^{\text{post}} = t_{k,i} - t_{k,j} \ \forall i, j \in N\,. \tag{10}$$

In other words, the delay between two spikes from two different neurons (i, j) should be identical between pattern k and m after moving the spikes. Substituting based on Eq. 9, this can be expressed as

$$(t_{m,i} - f_i) - (t_{m,j} - f_j) = t_{k,i} - t_{k,j}\,. \tag{11}$$

Let c_i be the shift in spike timing for each neuron in epoch m, such that the spike train patterns become identical,

$$c_i \equiv t_{m,i} - t_{k,i}\,. \tag{12}$$

Note that with this definition of c_i, the equation

$$(t_{m,i} - c_i) - (t_{m,j} - c_j) = t_{k,i} - t_{k,j} \tag{13}$$

holds for all (i, j). For all i, we can express f_i as a function of the shift c_i, such that

$$f_i \equiv c_i - g_i\,. \tag{14}$$

We wish to solve

$$\vec{g}_{\min} \equiv \arg\min_{\vec{g}} F_{km} = \arg\min_{\vec{g}} \sum_i^N |c_i - g_i| \tag{15}$$

under the constraint of Eq 11.
From Eqs 11, 13 and 14 it follows that

$$(t_{m,i} - c_i + g_i) - (t_{m,j} - c_j + g_j) = (t_{m,i} - c_i) - (t_{m,j} - c_j) \tag{16}$$

Hence the equation $g_i = g_j$ holds for all (i, j). Thus, we can rewrite Eq. 15 to

$$g^{\min} \equiv \arg\min_{g} \sum_i^N |c_i - g| \tag{17}$$

to find a global shift that minimizes the L1-norm of the residuals. The solution to this this equation is

$$g^{\min} = \text{Median}\{\vec{c}\}\,. \tag{18}$$

Thus, our main result is that the original shifts between the two spiking patterns can be written as the decomposition

$$c_i = g^{\min} + f_i\,, \tag{19}$$

for all i, i.e. the optimal transport in terms of neuron-specific shifts and a global temporal rigid translation term. Thus, the optimal transport between two spiking patterns (e.g. after stimulus onset) can be decomposed into the optimal transport in terms of neuron-specific shifts and a global temporal rigid translation term.

Global shift definition for multiple spikes

We now consider the case where in each epoch, every neuron fires a variable number of spikes. We will show that a similar derivation for SpikeShip can be made based on the weighted median. Let $n_{i,k}$ and $n_{i,m}$ be the number of spikes for the i-th neuron in epoch k and m. In the SPOTDis, we normalized the cross-correlations to unit mass, such that each spike effectively gets the same weight. For SpikeShip, we will also assign a weight to each spike, such that the total weight per neuron in the computation of SpikeShip is equal. In order to do so, we first find the smallest common multiple of the spike counts for each neuron, denoted n_i^*. For instance, if $n_{i,k} = 2$ and $n_{i,m} = 6$ then the least common multiple equals 6. We now replicate each spike $\frac{n_i^*}{n_{i,k}}$ and $\frac{n_j^*}{n_{i,m}}$ times. Each spike will now have a weight of $w_i \equiv \frac{1}{n_i^*}$. (Note that in the actual computation, we do not replicate the spikes in practice, but use an algorithm similar to the one detailed in [22]). Then, based on the optimal transport cost (EMD), we obtain shifts $c_{i,u}$ for the u-th spike of the i-th neuron, $u = (1, \ldots, n_i^*)$. Note that computation of the EMD amounts to shifting the most left-ward spike (i.e. first spike) out of n_i^* spikes in epoch m to the most left-ward spike in epoch k [22].

We use a similar derivation as the one above. Let $t_{m,i,u}$ be the timing of the $u-th$ replicated spike for neuron i in the mth epoch, for all (i, m, u), $u = (1, \ldots, n_i^*)$. We denote the spike times after (post) moving them in epoch m as

$$t_{m,i,u}^{\text{post}} \equiv t_{m,i,u} - f_{i,u} \tag{20}$$

$\forall (i, u)$, where we omitted the subscripts k, m from the variable $f_{i,km,u}$ for simplicity. The constraint that all the across-neuron spike timing relationships should be identical after moving implies that

$$t_{m,i,u}^{\text{post}} - t_{m,j,u}^{\text{post}} = t_{k,i,u} - t_{k,j,u} \tag{21}$$

In other words, the delay between two spikes from two different neurons (i, j) should be identical between pattern k and m after moving the spikes. Substituting based on Eq. 20, this can be expressed as

$$(t_{m,i,u} - f_{i,u}) - (t_{m,j,u} - f_{j,u}) = t_{k,i,u} - t_{k,j,u}\,. \tag{22}$$

There is one additional constraint, namely

$$(t_{m,i,u} - f_{i,u}) - (t_{m,i,v} - f_{i,v}) = t_{k,i,u} - t_{k,i,v}\,. \tag{23}$$

In other words, all the pairwise relationships after moving within the same neuron should be identical.

Let $c_{i,u}$ be the shift in spike timing for each neuron in epoch m, such that the spiking patterns in the window become identical,

$$c_{i,u} \equiv t_{m,i,u} - t_{k,i,u}\,. \tag{24}$$

Note that with this definition of $c_{i,u}$, the equation

$$(t_{m,i,u} - c_{i,u}) - (t_{m,j,u} - c_{j,u}) = t_{k,i,u} - t_{k,j,u} \tag{25}$$

holds for all (i, j, u). For all i, u, we can express $f_{i,u}$ as a function of the shift $c_{i,u}$, such that

$$f_{i,u} \equiv c_{i,u} - g_{i,u}\,. \tag{26}$$

Define $\vec{g} \equiv \left(\left(g_{i,1}, \ldots, g_{i,n_i^*}\right), \ldots, \left(g_{N,1}, \ldots, g_{N,n_N^*}\right)\right)$.

We wish to solve

$$\vec{g}_{\min} \equiv \arg\min_{\vec{g}} \sum_{i}^{N} \sum_{u}^{n_i^*} w_{i,u} |c_{i,u} - g_{i,u}| \tag{27}$$

under the constraints of Eq 22, 23 and 25.

Given these two constraints, the equation $g_{i,u} = g_{j,u}$ holds for all (i, j, u). Thus, we can rewrite Eq. 27 to

$$g^{\min} \equiv \arg\min_{g} \sum_{i}^{N} \sum_{u}^{n_i^*} w_{i,u} |c_{i,u} - g| \tag{28}$$

to find a global translation term that minimizes the L1-norm of the residuals. The solution to this this equation is the weighted median g,

$$g^{\min} = \text{WeightedMedian}\left(\left(c_{1,1}, w_{i,u}, \ldots, c_{1,n_1^*}, w_{1,n_1^*}\right), \ldots, \left(c_{N,1}, w_{N,1}, \ldots, c_{N,n_N^*}, w_{N,n_N^*}\right)\right) .$$

Now average mover cost, *SpikeShip*, equals

$$F_{km} \equiv \frac{1}{|\mathcal{A}_{km}|} \sum_{i \in \mathcal{A}_{km}} \frac{1}{n_i^*} \sum_{u}^{n_i^*} |f_{i,u}| \,. \tag{29}$$

where $\mathcal{A}_{km} \equiv \{i : n_{i,m} > 0 \wedge n_{i,k} > 0\}$ is the set of neurons that are active in both epochs k and m. Thus, we derive the result that the original shifts between the two spiking patterns can be written as the decomposition

$$c_{i,u} = g^{\min} + f_{i,u} \,, \tag{30}$$

for all (i, u), i.e. the optimal transport in terms of neuron-specific shifts and a global translation term. Thus, the optimal transport between two spiking patterns (e.g. after stimulus onset) can be decomposed into the optimal transport in terms of neuron-specific shifts and a global temporal rigid translation term. This computation has linear complexity $\mathcal{O}(N)$. We base the computation of the weighted median on [31, 32] and an adaptation of the *Robustats* [33] Python library. In practice, the computation of $c_{i,u}$ (optimal transport per neuron) can be efficiently performed not by replicating the spikes to the common multiple integer (used in derivation above), but by using a similar algorithm as in [22].

Relationship SpikeShip and SPOTDis

We now derive an analytical relationship between SpikeShip and SPOTDis, for the case of uniform sequences in which each neuron fires only at one time point of the sequence; note that this result does not generalize to more complex distributions, or the case of multiple spikes. We note that the pairwise distance among the cross-correlation for four spikes (neuron i and j, epoch k and m) equals $|(t_{m,i} - t_{m,j}) - (t_{k,i} - t_{k,j})| = |c_i - c_j|$. For simplicity we define SPOTDis over all N^2 elements (note the distance of an element with itself equals zero) and assume that all neurons fire a spike, without loss of generalization. From Eq. 31 we can rewrite the SPOTDis as

$$\begin{aligned} D_{km} &\equiv \frac{1}{N^2} \sum_{i,j} |c_i - c_j| \\ &= \frac{1}{N^2} \sum_{i,j} |f_i - f_j| \,. \end{aligned} \tag{31}$$

We have as expected value $\mathbb{E}\{D_{km}\} = \mathbb{E}\{|f_i - f_j|\}$. Because we defined $f_i = c_i - g^{\min}$, where $g^{\min} = \text{Median}\{\vec{c}\}$, we know that the median of our distribution is zero. We can thus assess the relationship between SpikeShip and SPOTDis for different distributions of f_i. We can divide the set of N (assuming N is even, without loss of generalization) neurons into two sets, namely $\mathcal{I}$ and $\mathcal{J}$, with $\mathcal{I} \equiv \{i : f_i \leq 0\}$ and $\mathcal{J} \equiv \{i : f_i \geq 0\}$. For the combinations (i, j) for which $i \in \mathcal{I}$ and $j \in \mathcal{J}$ we obtain the contribution to SPOTDis as

$$\begin{aligned} D_{km}^{pos,neg} &= \frac{1}{2}\,\mathbb{E}\{|f_i - f_j|\} \\ &= \frac{1}{2}\,\mathbb{E}\{|f_j| + |f_i|\} \\ &= \mathbb{E}\{F_{km}\} \end{aligned} \tag{32}$$

where the factor $\frac{1}{2}$ reflects the probability of f_i and f_j having opposite signs. Thus, the term $D_{km}^{pos,neg}$ does not depend on the specific distribution of the spikes.

For the combinations (i, j) for which $i \in \mathcal{I}$ and $j \in \mathcal{J}$ the expected distance depends on the distribution of f_i. If we assume that the different spike patterns each uniformly cover a window length of $2T$, then we know that f_i will have a triangular probability distribution, i.e.

$$p(f_i) = \frac{T - |f_i|}{T^2}\,, -T \leq f_i \leq T\,. \tag{33}$$

We now obtain

$$\mathbb{E}\{D_{km}^{pos,pos} + D_{km}^{neg,neg}\} = \frac{1}{2}\int_0^T \int_0^{f_i} 8\frac{T - f_i}{T^2}\frac{T - f_j}{T^2}(f_i - f_j)\,df_j\,df_i = \frac{2T}{15} \tag{34}$$

Note that for this distribution we also have $\mathbb{E}\{|f_i|\} = \frac{T}{3}$. Hence,

$$\mathbb{E}\{D_{km}\} = \mathbb{E}\left\{\left(1 + \frac{2}{5}\right)F_{km}\right\}\,. \tag{35}$$

Thus, the average amount of transport on the individual spikes is smaller ($\frac{5}{7}$) than the average transport on the pairs of spikes.

Application in high-dimensional neural data

Allen Brain Institute datasets

We used the free, public available datasets of Allen Brain Institute through AllenSDK (For more details, see http://help.brain-map.org/display/observatory/Documentation). Neuropixels silicon probes [9] were used to record neurons with precise spatial and temporal resolution [12].

We selected the cells of 32 mice during natural scenes presentations. The cells were selected considering a signal-noise ratio (SNR) such that $SNR > 0$. The neural activity from a total of $N = 8,301$ cells were selected from the Primary visual area (VISp), Lateral visual area (VISl), Anterolateral visual area (VISal), Posteromedial visual area (VISpm), Rostrolateral visual area (VISrl), and Anteromedial visual area (VISam).

Spontaneous activity

For the spontaneous activity dataset, we used free, public available datasets [23]. It contains data about three mice: "Waksman" ($N = 2,688$), "Robbins"($N = 2,296$),

and "Krebs" ($N = 1,462$). Probes were located in distinct cortical areas (visual, sensorimotor, frontal, and retrosplenial), hippocampus, thalamus, striatum, and midbrain [10]. Furthermore, each experiment has information about the recorded spike times, cells, and the processed SVD components of whisker's motion (i.e. pixel difference between consecutive frames of a mouse face movie).

For our analyzes, we added the first four SVD components (Fig. 6A) and then we subtracted the median across dimensions (denoising, see Fig. 6B). A sliding window was used to sum the activity SVD whisker's motion across the interval $[t, t + 0.5]$ seconds (Fig. 6C,D). We selected one hundred epochs for both low- and high-motion states based on the SVD motion value, and ran SpikeShip across different amounts of cells, depending of the experiment. The manifold learning algorithm were t-SNE and Spectral Embedding from the python library Scikit Learn v0.22.1.

Discriminability index

Since information in temporal spiking sequences compared to the information from traditional firing rate codes could differ, we wanted to quantify to what extent the degree of discriminability within and between different visual stimuli differ in a dissimilarity matrix $diss$ (i.e. within and between natural images) per stimulus id .

To this end, we computed a "Discriminability index" (d), defined as the difference between the average distance within and between stimulus id, divided by the squared sum of their variances to the power of two.

$$d_{diss,id} = \frac{\mu_{diss,between,id} - \mu_{diss,within,id}}{\sqrt{s^2_{diss,between} + s^2_{diss,within}}} \tag{36}$$

Therefore, it indicates how many standard deviations are two set of distances away from each other.

Acknowledgements

This project was financed by the BMF (Bundesministerium fuer Bildung und Forschung), Computational Life Sciences, project BINDA (031L0167).

Authorship Contributions

Conception and problem statement: BSG, FPB, MV. Data analysis and simulations: BSG. Mathematical analysis: BSG and MV. Supervision: MV. Writing of main draft: BSG and MV.

Supporting information

References

1. Havenith MN, Yu S, Biederlack J, Chen NH, Singer W, Nikolic D. Synchrony makes neurons fire in sequence, and stimulus properties determine who is ahead. J Neurosci. 2011;31(23):8570–84.

2. Vinck M, Lima B, Womelsdorf T, Oostenveld R, Singer W, Neuenschwander S, et al. Gamma-phase shifting in awake monkey visual cortex. Journal of Neuroscience. 2010;30(4):1250–1257.

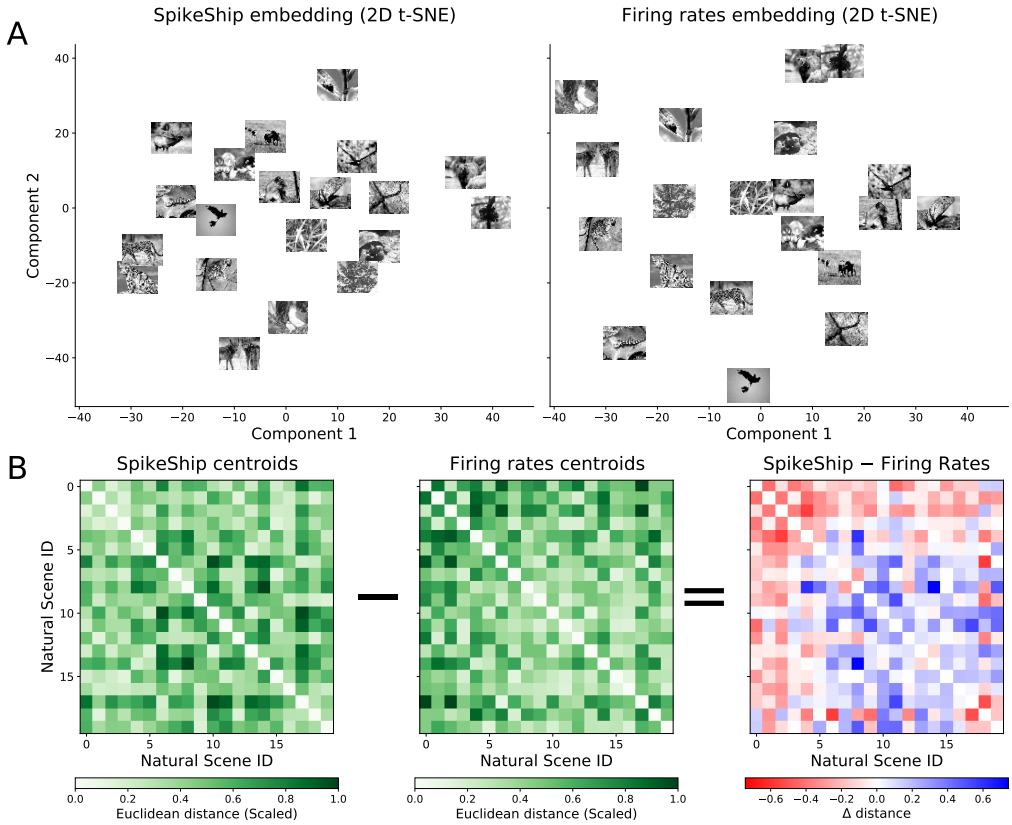

Fig 7. Comparison between clusters from SpikeShip and Firing rates embeddings of Natural scenes. A) 2D t-SNE embeddings from SpikeShip and Firing rates' dissimilarity matrices. Allocation of natural scenes' clusters are different between the two embeddings. B) Scaled euclidean pairwise distance between centroids of each cluster for both SpikeShip (Left) and Firing rates (Middle), and their difference (Right).

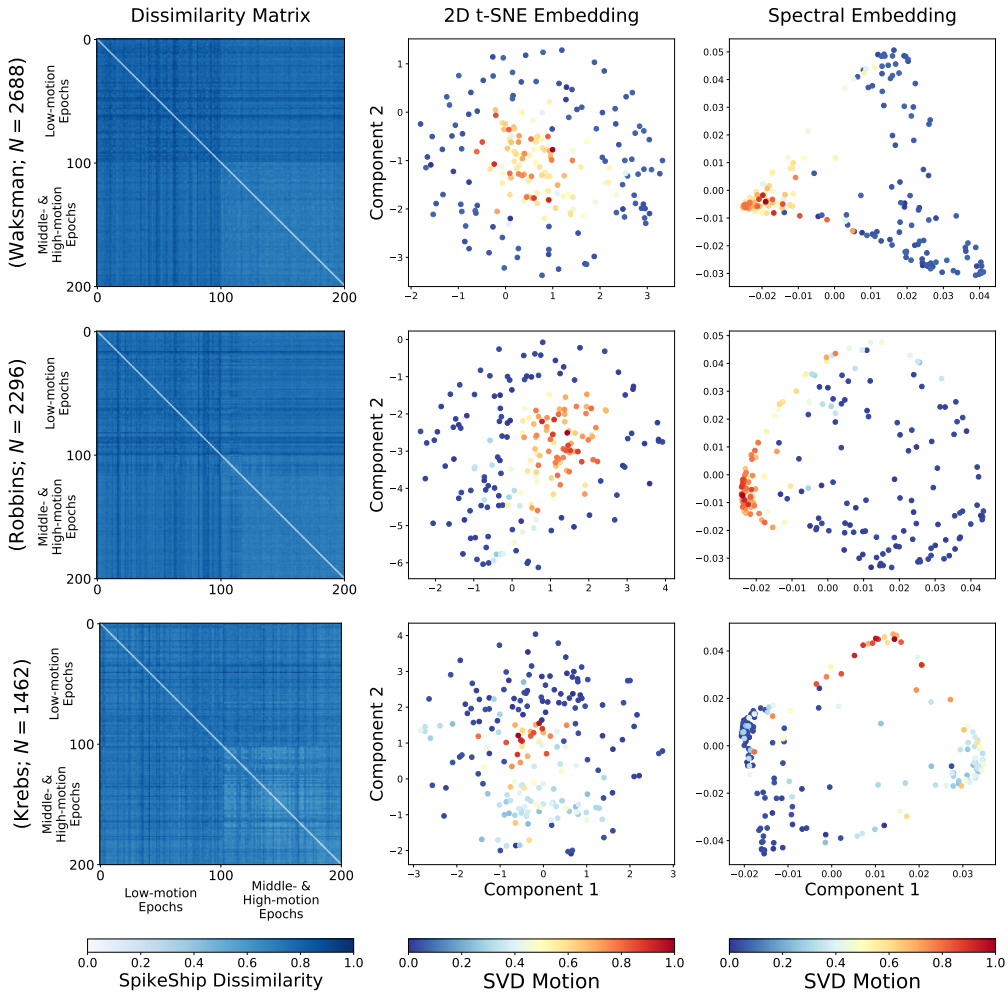

Fig 8. Spontaneous activity analyzes for 3 mice. Multi-spike sequence analyzes for three mice (rows). Left: dissimilarity matrices. Middle: 2D t-SNE embedding. Right: 2D Spectral Embedding (Laplacian Eigenmaps).

3. Luczak A, Bartho P, Harris KD. Spontaneous events outline the realm of possible sensory responses in neocortical populations. Neuron. 2009;62(3):413–25.

4. Lu T, Liang L, Wang X. Temporal and rate representations of time-varying signals in the auditory cortex of awake primates. Nat Neurosci. 2001;4(11):1131–8.

5. Pastalkova E, Itskov V, Amarasingham A, Buzsaki G. Internally generated cell assembly sequences in the rat hippocampus. Science. 2008;321(5894):1322–7.

6. Ikegaya Y, Aaron G, Cossart R, Aronov D, Lampl I, Ferster D, et al. Synfire chains and cortical songs: temporal modules of cortical activity. Science. 2004;304(5670):559–564.

7. Wehr M, Laurent G. Odour encoding by temporal sequences of firing in oscillating neural assemblies. Nature. 1996;384(6605):162–6.

8. Seung HS, Lee DD. The manifold ways of perception. science. 2000;290(5500):2268–2269.

9. Jun JJ, Steinmetz NA, Siegle JH, Denman DJ, Bauza M, Barbarits B, et al. Fully integrated silicon probes for high-density recording of neural activity. Nature. 2017;551(7679):232–236.

10. Stringer C, Pachitariu M, Steinmetz N, Reddy CB, Carandini M, Harris KD. Spontaneous behaviors drive multidimensional, brainwide activity. Science. 2019;364(6437).

11. Stringer C, Michaelos M, Tsyboulski D, Lindo SE, Pachitariu M. High-precision coding in visual cortex. Cell. 2021;184(10):2767–2778.

12. Siegle JH, Jia X, Durand S, Gale S, Bennett C, Graddis N, et al. Survey of spiking in the mouse visual system reveals functional hierarchy. Nature. 2021;592(7852):86–92.

13. Chang L, Tsao DY. The code for facial identity in the primate brain. Cell. 2017;169(6):1013–1028.

14. Churchland MM, Cunningham JP, Kaufman MT, Foster JD, Nuyujukian P, Ryu SI, et al. Neural population dynamics during reaching. Nature. 2012;487(7405):51–56.

15. Dragoi G, Buzsaki G. Temporal encoding of place sequences by hippocampal cell assemblies. Neuron. 2006;50(1):145–57.

16. Mainen ZF, Sejnowski TJ. Reliability of spike timing in neocortical neurons. Science. 1995;268(5216):1503–1506.

17. Markram H, Lubke J, Frotscher M, Sakmann B. Regulation of synaptic efficacy by coincidence of postsynaptic APs and EPSPs. Science. 1997;275(5297):213–5.

18. Dan Y, Poo MM. Spike timing-dependent plasticity of neural circuits. Neuron. 2004;44(1):23–30.

19. Abbott LF, Blum KI. Functional significance of long-term potentiation for sequence learning and prediction. Cereb Cortex. 1996;6(3):406–16.

20. Buonomano DV, Maass W. State-dependent computations: spatiotemporal processing in cortical networks. Nat Rev Neurosci. 2009;10(2):113–25.

21. Singer W, Lazar A. Does the cerebral cortex exploit high-dimensional, non-linear dynamics for information processing? Frontiers in computational neuroscience. 2016;10:99.

22. Grossberger L, Battaglia FP, Vinck M. Unsupervised clustering of temporal patterns in high-dimensional neuronal ensembles using a novel dissimilarity measure. PLoS computational biology. 2018;14(7):e1006283.

23. Steinmetz N, Pachitariu M, Stringer C, Carandini M, Harris K. Eight-probe Neuropixels recordings during spontaneous behaviors; 2019. Available from: `https://janelia.figshare.com/articles/dataset/Eight-probe_Neuropixels_recordings_during_spontaneous_behaviors/7739750/4`.

24. Van der Maaten L, Hinton G. Visualizing data using t-SNE. Journal of machine learning research. 2008;9(11).

25. Van Der Maaten L. Accelerating t-SNE using tree-based algorithms. The Journal of Machine Learning Research. 2014;15(1):3221–3245.

26. McInnes L, Healy J, Astels S. hdbscan: Hierarchical density based clustering. The Journal of Open Source Software. 2017;2(11).

27. Thorpe S, Delorme A, Van Rullen R. Spike-based strategies for rapid processing. Neural networks. 2001;14(6-7):715–725.

28. McGinley MJ, Vinck M, Reimer J, Batista-Brito R, Zagha E, Cadwell CR, et al. Waking State: Rapid Variations Modulate Neural and Behavioral Responses. Neuron. 2015;87(6):1143–61.

29. Williams AH, Poole B, Maheswaranathan N, Dhawale AK, Fisher T, Wilson CD, et al. Discovering precise temporal patterns in large-scale neural recordings through robust and interpretable time warping. Neuron. 2020;105(2):246–259.

30. Resulaj A, Ruediger S, Olsen SR, Scanziani M. First spikes in visual cortex enable perceptual discrimination. Elife. 2018;7:e34044.

31. Cormen TH, Leiserson CE, Rivest RL, Stein C. Introduction to algorithms. MIT press; 2009.

32. Bleich C, Overton ML. A linear-time algorithm for the weighted median problem. Courant Institute of Mathematical Sciences, New York University; 1983.

33. Bovo F. Robustats; 2020. `https://github.com/FilippoBovo/robustats`.